Research Square

Preprints are preliminary reports that have not undergone peer review.
They should not be considered conclusive, used to inform clinical practice,
or referenced by the media as validated information.

Metabolic Signatures after Endoscopic Sleeve Gastroplasty (ESG) Versus Natural Orifice Trans-luminal Endoscopic Surgical Gastric Bypass (NOTES-GB): A Surviving Porcine Study

Chin Hong Lim

lim.chin.hong@singhealth.com.sg

Singapore General Hospital

Ciaran Jian Bo Lim

Singapore General Hospital

Koy Min Chue

Sengkang General Hospital

Nan Guang Tan

Singapore General Hospital

Baldwin Po Man Yeung

Sengkang General Hospital

Jin Lin Lin

Changi General Hospital

Lester Wei Lin Ong

Sengkang General Hospital

Weng Hoong Chan

Singapore General Hospital

Ravishankar Asokkumar

Singapore General Hospital

Jeremy Tian Hui Tan

Singapore General Hospital

Research Article

Keywords:

Posted Date: May 4th, 2026

DOI: https://doi.org/10.21203/rs.3.rs-9213853/v1

License: This work is licensed under a Creative Commons Attribution 4.0 International License.
Read Full License

Additional Declarations: No competing interests reported.

Abstract

Introduction

Bariatric surgery improves metabolic outcomes in obesity and type 2 diabetes mellitus (T2DM), yet widespread adoption is limited by the invasiveness and morbidity of conventional laparoscopic approaches. Patient preference for less invasive options has driven the development of endoscopic bariatric therapies (EBTs). Intragastric balloons and endoscopic sleeve gastroplasty (ESG) reduce weight but show more modest metabolic benefits and limitations in durability and remission. We developed natural orifice transluminal endoscopic surgery-gastric bypass (NOTES-GB), a novel NOTES-based intestinal bypass approach designed to replicate key bypass-associated metabolic effects through flexible endoscopy. This study aimed to define system-wide metabolic changes after NOTES-GB vs ESG relative to controls using untargeted metabolomics, hypothesizing that both procedures would significantly reshape the metabolome and that procedure-specific signatures would emerge.

Methods

Thirteen adolescent castrated male pigs were randomized to receive ESG, NOTES-GB, or control. Blood was collected at baseline and 7 months post-intervention. Untargeted UPLC-MS/MS metabolomics was performed in positive and negative ion modes. Differential metabolites were assessed using PCA, volcano plots, Venn-based comparisons, pathway enrichment analyses, and Pearson correlation (significance threshold $P < 0.05$) to evaluate coordinated metabolite networks.

Results

We identified 1487 positive and 785 negative ion-mode metabolites. In positive ion mode, NOTES-GB produced more differential metabolites than ESG: 536 in NOTES-GB vs CONTROL (162 up, 374 down) compared with 194 in ESG vs CONTROL (98 up, 96 down). Key discriminating metabolites included N-acetylcitrulline, 1-(β-D-ribofuranosyl)-1,4-dihydronicotinamide, benzoylagmatine, cis-zeatin, and fissoldhimine. Pathways differed: ESG was enriched in digestive/endocrine and amino-acid metabolism, whereas NOTES-GB showed enrichment in lipid metabolism and cofactor/vitamin-related pathways, alongside amino-acid metabolism. Correlation analysis supported coordinated metabolite network regulation.

Discussion & Conclusion

NOTES-GB induced broader metabolomic remodeling than ESG, consistent with greater disruption of nutrient routing and gut–host metabolic communication. Procedure-specific pathway enrichment i.e. digestive/endocrine signaling for ESG versus lipid and cofactor/vitamin networks for NOTES-GB suggests distinct mechanisms underpinning metabolic effects. These metabolomic signatures may help explain why intestinal bypass approaches achieve stronger systemic metabolic remodeling than restrictive strategies.

Introduction

Bariatric surgery has markedly transformed the management of obesity and type 2 diabetes mellitus (T2DM) over the past several decades. Long-term data from the Swedish Obese Subjects (SOS) study demonstrated that Roux-en-Y gastric bypass (RYGB) resulted in an average sustained total body weight loss of approximately 25% at ten years [1]. Similarly, findings from the STAMPEDE trial showed that 51% of patients undergoing gastric bypass achieved remission of T2DM at five years, significantly surpassing outcomes observed with intensive medical therapy alone [2]. These sustained improvements in glycemic control have been associated with meaningful reductions in diabetes-related complications and mortality.

Despite robust clinical benefits, bariatric surgery remains significantly underutilized in North America. Only about 1% of individuals who meet eligibility criteria ultimately undergo surgery, in part due to concerns about perioperative risks, including a reported mortality rate of 0.5–1%, as well as complications linked to conventional laparoscopic techniques [3]. This gap between eligibility and uptake highlights a substantial unmet need. Notably, survey data suggest that nearly 80% of patients in the United States express a preference for incisionless treatment options, emphasizing the demand for safer and less invasive therapeutic strategies [4].

Endoscopic bariatric therapies (EBTs) have emerged as minimally invasive alternatives that avoid surgical incisions by using a transoral endoscopic approach. The most widely adopted EBTs include intragastric balloons and endoscopic sleeve gastroplasty (ESG). These techniques either occupy space within the stomach or use endoluminal suturing to reduce gastric capacity. On average, they produce total body weight loss in the range of 10–14%, although rates of T2DM remission are generally lower than those achieved with gastric bypass procedures [5]. Questions remain regarding long-term durability. Intragastric balloons require removal within 12 months, and ESG has been associated with an approximate 17% rate of suture failure at one year [6]. Importantly, the long-term metabolic benefits of surgical gastric/intestinal bypass (e.g., RYGB or OAGB) are mediated not only by mechanical effects but also by profound alterations in gut-driven regulation of glucose metabolism. By bypassing the duodenum and proximal jejunum, these procedures prevent nutrient-triggered “anti-incretin signals,” thereby improving hormonal changes that support insulin secretion and sensitivity. Metabolomic and lipidomic profiling can be used to gain a deeper understanding of the molecular mechanisms by which bariatric surgery leads to improved metabolic health. Previous studies have reported post-surgical changes in multiple metabolites, including amino acids, lipids, bile acids, and known cardiometabolic disease markers including branched-chain amino acids (BCAAs) and trimethylamine-N-oxide (TMAO) [7, 8].

To address the clinical need for a minimally invasive bypass strategy, we developed NOTES-GB, a novel NOTES-based gastric bypass designed to replicate key metabolic effects of gastric bypass using flexible endoscopy. We previously demonstrated feasibility and reported successful outcomes of NOTES-GB in porcine and cadaveric models [9, 10]. In our recent published surviving animal study, NOTES-GB produced greater weight loss than ESG [11]. The primary aim of this study is to determine system-wide

metabolic changes induced by restrictive ESG versus intestinal bypass via NOTES-GB, in patterns analogous to those observed in bariatric surgery. We performed untargeted metabolomic profiling on blood samples collected from animals randomized to receive ESG or NOTES-GB, and hypothesized that both interventions would substantially alter the metabolome relative to controls, while producing distinct, procedure-specific metabolic signatures independent of weight.

Material and Methods

1. Animal Preparation

Thirteen adolescent, castrated male domestic pigs (Sus scrofa domesticus), weighing 30–40 kg, were included in this study. All animals were managed in accordance with SingHealth Duke-NUS institutional guidelines and were acclimated for a minimum of seven days at the SIMS facility prior to any intervention. Housing conditions were standardized, with an ambient temperature maintained at 25°C and a 12-hour light–dark cycle. Animals had unrestricted access to water, and stalls were cleaned daily. To establish a diet-induced obesity model, pigs were provided a specially formulated high-calorie diet twice per day for three months. The obesogenic feed was enriched in fructose, fat, and cholesterol and consisted of 16.1% protein, 43.1% fat, and 40.8% carbohydrate, delivering approximately 3,580 kcal per feeding (7,160 kcal/day total). Following the dietary induction period, animals were assigned to experimental groups based on procedural intervention. Two pigs underwent sham upper endoscopy and served as controls. Two animals received endoscopic sleeve gastroplasty (ESG), while the remaining nine underwent natural orifice transluminal endoscopic surgery gastric bypass (NOTES-GB) to evaluate procedure-specific outcomes.

2. Ethical Considerations and Animal Welfare

All procedures were performed in accordance with institutional and national regulations for animal research following formal protocol review to ensure scientific justification and the lack of suitable alternatives. Animal welfare was prioritized throughout the study by implementing measures to minimize pain and distress, maintaining appropriate housing and nutrition, and providing ongoing veterinary oversight. All interventions were conducted by trained personnel experienced in humane animal care to ensure ethical standards were upheld while achieving the study objectives.

3. Endoscopic Intervention

The NOTES-GB procedure was performed as previously described [11]. Anesthesia was induced with intramuscular ketamine (22 mg/kg) and atropine (0.005 mg/kg), followed by intravenous sodium pentobarbital (10 mg/kg). After intubation (6.0-Fr soft-cuff), animals were mechanically ventilated with 2.0% isoflurane in oxygen. In the supine position with an esophageal overtube in place, a 5-mm anterior antral gastrostomy was created using an ultra-slim gastroscope. A jejunal loop was identified

endoscopically, an enterotomy was made under fluoroscopic guidance, and a 450-cm guidewire was advanced and externalized orally. A 20-mm HOT Axios LAMS was deployed to create the gastrojejunostomy and dilated to 20 mm. Full-thickness endoscopic suturing (OverStitch, 2/0 polypropylene) was performed to reinforce the anastomosis and close the pylorus, and leak testing was completed with contrast.

Postoperatively, morphine (0.5 mg/kg SC) and amoxicillin (15 mg/kg) were administered. Animals resumed water overnight, advanced to a mixed diet for three weeks, and were titrated to target caloric intake by postoperative day 5. The LAMS was removed endoscopically at 24 weeks, followed by reassessment at week 28 and necropsy to evaluate anastomotic patency, mucosal integrity, lumen diameter, and suture durability.

4. Analysis of Circulating Biomarkers

Plasma levels of ALP, ALT, AST, GLDH, total cholesterol (TC), triglycerides (TG), glucose (GLU), insulin, C-peptide, GLP-1, fructosamine (FRA), and albumin (ALB) were measured using porcine-specific commercial assay/ELISA kits (Leadman, Beijing, China) per manufacturer instructions. Blood was collected aseptically from the marginal ear vein or external jugular vein. To reduce local injury, no more than three sampling attempts were allowed; local anesthetic cream was applied 30 minutes prior to collection. The external jugular vein was used if > 5 mL was required.

5. Analysis of Metabolites

Untargeted metabolomics was performed on baseline and 7-month post-intervention samples using UPLC-MS/MS (positive and negative ion modes) and hydrophilic interaction chromatography/UPLC-MS/MS in negative mode. Samples were processed using a MicroLab STAR system. After methanol extraction to remove proteins, metabolites were analyzed by UPLC-MS/MS. Raw data were extracted and quality-checked, and compounds were identified by matching against purified standard library entries using retention time/index, m/z, and MS/MS spectral features.

6. Statistical & Bioinformatics Analysis

Normality was assessed with the Shapiro–Wilk test. Data were summarized as mean ± standard deviation. One-way ANOVA (SPSS) compared group differences; ANCOVA was used to evaluate procedure effects across weeks 4–28 while controlling for week 0 baseline, and across weeks 0–28 while controlling for week 24. Raw MS data were converted to mzXML using ProteoWizard [3], followed by peak detection, alignment, and retention-time correction with XCMS [4]. Peak areas were normalized within samples; metabolites with > 50% missing values across groups were removed. Identification results were matched to the Novogene local database and filtered by metabolite coefficient of variation (CV) ≤ 30%. Multivariate analyses (PCA, PLS-DA) were performed to distinguish metabolic patterns

between groups, and hierarchical clustering (HCA) plus metabolite correlation analysis were used to explore sample-to-sample and metabolite-to-metabolite relationships. Pathway enrichment analyses were applied to interpret biological relevance.

Results

All the animals underwent successful ESG & NOTES for gastrointestinal bypass procedure. The mean weight of the animals was 34.7 kg (range: 29-40 kg), and the mean procedure time was 215.4 minutes (range: 180-255 minutes). Different weight trajectories were observed among the animals, as illustrated in **Figure 1**. Compared to the control and ESG groups, the NOTES-GB group exhibited significant weight differences at weeks 4 and 28, although this analysis excludes three animals that did not reach the study endpoint. After adjusting for week 24, there was a statistically significant difference in week 28 between the procedure groups P = 0.013. This large effect size indicates that the procedure accounted for 76.7% of the variance in weight at week 28 after controlling for week 24. Unfortunately, the significant differences in weight diminished between weeks 4 and 24.

One case of LAMS migration was detected during the planned X-ray at 3 months. The migration occurred without overt clinical symptoms and was successfully corrected endoscopically. Another pig died suddenly on postoperative day 6. Prior to death, the animal showed poor oral intake; necropsy revealed ischemic bowel due to mesenteric volvulus. This risk may be heightened in the porcine model due to a longer and highly mobile mesentery, which predisposes to volvulus during endoscopic gastrojejunostomy.

Two additional animals were euthanized prematurely due to severe weight loss (>30% below the expected growth rate over 2 weeks), despite assisted feeding and intravenous hydration. The euthanasia decision was made by the attending veterinarian in consultation with the research team. These animals were excluded from biomarker and metabolomic analyses.

Among serum biomarkers, most showed no significant longitudinal changes, with the exception of fasting GLP-1 (**Table 1**). GLP-1 levels in the control and ESG groups tended to decrease over time, whereas the NOTES-GB group showed an increase (**Figure 2**). This between-group difference was statistically significant ($P < 0.011$).

There were significant changes in plasma metabolites at baseline and 7-months following the endoscopic interventions. Untargeted metabolomics identified 1487 metabolites in positive ion mode and 785 in negative ion mode. In the positive ion mode, 536 metabolites differed significantly in the NOTES-GB versus control comparison (162 upregulated, 374 downregulated), whereas 194 metabolites differed in the ESG versus control comparison (98 upregulated, 96 downregulated). Overall, NOTES-GB produced a greater magnitude of metabolite alteration than ESG.

Principal component analysis (PCA) transformed correlated metabolite variables into orthogonal components, enabling dimensionality reduction and visualization of overall metabolic differences and

within-group variability (**Figure 3**). Volcano plots summarized differential metabolites, where the x-axis indicates log2 fold change and the y-axis indicates (-log10 (P-value). Red and blue dots represent significantly upregulated and downregulated metabolites, respectively, with dot size reflecting VIP values (**Figure 4**). Venn diagrams further illustrated overlaps and unique differences in the sets of differential metabolites across comparisons (**Figure 5**). A matchstick plot highlighted directionality and effect sizes among the top changing metabolites (**Figure 6**). The five metabolites with the largest changes in ESG and NOTES-GB relative to control were N-acetylcitrulline, 1-(β-D-ribofuranosyl)-1,4-dihydronicotinamide, benzoylagmatine, cis-zeatin, and fissoldhimine.

In pathway enrichment analyses, we revealed divergent metabolic pathway signatures between ESG and NOTES-GB compared with control. ESG was most enriched in digestive and endocrine system pathways, as well as amino acid metabolism. In contrast, NOTES-GB showed enrichment in lipid metabolism, cofactor and vitamin-related pathways, and pathways associated with amino acid metabolism (**Figure 7**).

Finally, differential metabolite correlation analysis assessed whether metabolite changes followed consistent (synergistic) or opposing (mutually exclusive) directions. Pearson correlation coefficients quantified relationships between metabolites, with values approaching 1 indicating positive correlation and values approaching −1 indicating negative correlation. Statistical significance was determined using P-value < 0.05 (**Figure 8**).

Discussion

Our understanding of gut physiology has advanced significantly in the last decade. We have moved away from viewing weight loss solely as a result of mechanical restriction and malabsorption, recognizing instead the complex physiological changes involved, such as alterations in gut neuroendocrine signalling, gastrointestinal motility, the autonomic nervous system, bile acid production, gut microbiota and metabolomic [12–14]. These factors contribute not only to weight loss but also to improvements in Type II diabetes mellitus.

To address the need for a minimally invasive gastric/intestinal bypass procedure, we developed the OAGB using the NOTES approach. Following successful trials in porcine and cadaveric models, we carried out untargeted metabolomic analysis to identify pathways and metabolites associated with changes in glucose homeostasis using a porcine sample after ESG, NOTES-GB, and CONTROL. In this study, we investigated metabolomic alterations following two bariatric procedures with distinct mechanisms: NOTES-GB, characterized by intestinal bypass, and ESG, characterized by a restrictive approach, compared with a CONTROL group. Across the identified metabolites in both positive and negative ion modes, we observed that NOTES-GB produced a greater overall impact on metabolite changes than ESG, as reflected by a higher number of differential metabolites in the NOTES-GB vs CONTROL comparison relative to the ESG vs CONTROL comparison. These findings suggest that the magnitude of systemic metabolic remodeling is closely related to the degree of disruption in nutrient

handling and gut–host interactions inherent to each procedure. While restriction primarily limits caloric intake and may modify endocrine signaling associated with satiety and digestion, intestinal bypass more strongly alters nutrient routing, luminal exposure, and absorption dynamics, which likely triggers broader downstream metabolic adaptations.

Consistent with this global remodeling, we identified several metabolites showing prominent changes after surgery, including N-acetylcitrulline, 1-(β-D-ribofuranosyl)-1,4-dihydronicotinamide, benzoylagmatine, cis-zeatin, and fissoldhimine. These metabolites collectively point to coordinated involvement of multiple biochemical networks. For example, metabolites associated with the arginine–citrulline and arginine-derived nitrogen metabolism axis (such as N-acetylcitrulline and benzoylagmatine) suggest that nitrogen handling and related metabolic fluxes may be substantially altered following intestinal bypass. In addition, the presence of 1-(β-D-ribofuranosyl)-1,4-dihydronicotinamide indicates perturbations in cofactor and redox-associated metabolism, consistent with changes in nicotinamide/NAD-linked pathways that are central to energy metabolism and cellular redox balance. Furthermore, metabolites such as cis-zeatin and fissoldhimine likely reflect microbial or microbe-modulated biochemical activity, supporting the notion that bypass procedures may exert stronger effects on gut microbial-derived metabolite production and gut–system metabolic crosstalk. Following NOTES-GB in the porcine model, targeted metabolomic analysis identified several metabolites that were significantly down-regulated, including 2,8-dihydroxyquinoline-β-D-glucuronide, 2-hydroxyoctanedioic acid, and indole-3-propionic acid (IPA). These metabolites collectively point to reduced activity across interlinked pathways involving (i) Phase II glucuronidation/xenobiotic conjugation, as suggested by the glucuronidated quinoline derivative; (ii) lipid oxidation–associated dicarboxylic acid metabolism, consistent with the down-regulation of the hydroxylated octanedioic acid intermediate; and (iii) tryptophan–microbiome related indole metabolism, reflected by decreased IPA, a canonical indole metabolite derived from tryptophan. In addition, the observed down-regulation of metabolites associated with tryptophan, methionine, and histidine metabolism further supports a coordinated shift in host amino-acid metabolic networks after NOTES-GB, likely integrating altered microbial metabolism and hepatic/intestinal handling of aromatic and sulfur-containing amino acid–derived compounds.

Pathway enrichment analyses further reinforced the concept of procedure-specific metabolic signatures. In the ESG group, the most enriched pathways compared with CONTROL included digestive and endocrine system pathways in addition to amino acid metabolism, aligning with a restrictive mechanism that primarily affects digestive physiology and endocrine regulation and only secondarily influences amino acid-related metabolic processes. In contrast, NOTES elicited enrichment in lipid metabolism, digestive and metabolism of cofactors and vitamins, alongside amino acid metabolism, indicating a broader reprogramming of systemic metabolism that extends beyond amino acid handling to encompass lipid utilization and cofactor/vitamin-related networks. This divergence is consistent with the mechanistic distinction between the procedures: intestinal bypass is expected to impact both the gut microbial ecosystem and host metabolic processing to a greater extent than restriction alone, thereby driving wider metabolomic change.

Finally, correlation analysis among differential metabolites suggested that the observed metabolic changes are not isolated but are instead organized into interacting networks, in which metabolites may exhibit synergistic relationships when they share similar change directions, or mutually exclusive relationships when their trends diverge. By evaluating Pearson correlations and applying statistical significance criteria ($P < 0.05$), our results support the presence of coordinated metabolic regulation following surgery. Taken together, these metabolomic and pathway-level findings indicate that NOTES leads to more pronounced and multi-axis metabolic remodeling, involving nitrogen metabolism, NAD-linked cofactor networks, lipid-related pathways, and gut-associated bioactive metabolite signatures, whereas ESG appears to produce a narrower, more endocrine/digestive-associated metabolic profile. These results provide mechanistic insight into how different bariatric strategies may drive distinct systemic metabolic outcomes and may help identify metabolite features that better reflect metabolic response after intestinal bypass versus restriction.

In conclusion, NOTES-GB produced a broader and more pronounced metabolomic remodeling than ESG in porcine model, consistent with the greater disruption of nutrient routing and gut–host interactions inherent to intestinal bypass. The associated metabolite signatures indicate coordinated shifts across nitrogen/arginine-derived metabolism, NAD-linked redox/cofactor networks, lipid-related pathways, and gut- or microbe-associated bioactive metabolites, including reduced xenobiotic conjugation, lipid oxidation-linked dicarboxylic acid metabolism, and tryptophan-indole signaling. In contrast, ESG showed a comparatively narrower profile enriched primarily in digestive and endocrine-related pathways, reflecting a more restriction-dominant mechanism. Together, these findings support procedure-specific, network-level metabolic adaptation after bariatric surgery, with NOTES eliciting the more extensive systemic response.

Declarations

Author Contribution

LCH and CL prepared the manuscriptLCH, BY, LJL and RA designed the studyCKM, TNG, LO and JT performed the proceduresLCH, BY and LJL analysed the data

Ethics Approval Statement

This study involving animal subjects has been conducted in accordance with ethical guidelines. Written informed consent and approval from the Institutional Review Board (IRB) was deemed unnecessary given the nature of the study. All procedures were performed in compliance with relevant regulations to ensure the welfare of the animals involved.

References

1. Sjostrom L, Narbo K, Sjostrom D, et al. Effects of Bariatric Surgery on Mortality in Swedish Obese Subjects. NEJM. 2007;357:741–52.
2. Schauer P, Bhatt DL, Kirwan JP, et al. Bariatric surgery versus intensive medical therapy for diabetes-5-year outcomes. N Eng J Med. 2017;376:641–51.
3. ASMBS. Estimate of bariatric surgery numbers 2011–2017 Gainesville, FL. 2018. https://asmbs.org/resources/estimate-of-bariatric-surgery-numbers
4. Swanstorm LL, Volckmann E, Hungness E, et al. Patient attitudes and expectations regarding natural orifice transluminal endoscopic surgery. Surg Endosc. 2009;23(7):1519–25.
5. Li A, Lim E, Lim CH. Predictors of early removal of intragastric balloon due to intolerance: Insights from a multiethnic Asian cohort. Ann Acad Med Singap. 2024;53(9):551–61.
6. Pizzicannella M, Lapergola A, Fiorillo C, et al. Does endoscopic sleeve gastroplasty stand the test of time? Objective assessment of endoscopic ESG appearance and its relation to weight loss in a large group of consecutive patients. Surg Endosc. 2020;34:3696–705.
7. Guo K, Yu H, Lu J, et al. Decreased serum betatrophin levels correlate with improved fasting plasma glucose and insulin secretion capacity after Roux-en-Y gastric bypass in obese Chinese patients with type 2 diabetes: a 1 year follow-up. Surg Obes Relat Dis. 2016;12:1343–8.
8. Vaz M, Pereira SS, Monteiro MP. Metabolomic signatures after bariatric surgery- a systemic review. Rev Endocr Metab Disord. 2022;23:503–19.
9. Lim CH, Lee ZJ, Yeung B, et al. Natural orifice transluminal endoscopic one-anastomosis gastric bypass: a feasibility study using porcine model. Surg Endo. 2021;35(3):5842–51.
10. Lim CH, Lee ZJ, Lye T, et al. Natural Orifice Transluminal Endoscopic One-Anastomosis Gastric Bypass: a Feasibility Study Using Human Cadavers. Obes Surg. 2022;32(7):1–9.
11. Lim CH, Chong WM, Chee SSH, et al. Gastric bypass via natural orifice transluminal endoscopic surgical (NOTES) approach: a surviving porcine study. Obes Surg. 2026;35(11):4701–10.
12. Hickey MS, Pories WJ, MacDonald KG Jr, et al. A new paradigm for type 2 diabetes mellitus: could it be a disease of the foregut? Ann Surg. 1998;227:637–43.
13. Pories WJ, et al. Who would have thought it? An operation proves to be the most effective therapy for adult-onset diabetes mellitus. Ann Surg. 1995;222(3):339–50.
14. Rubino F, Forgione A, Cummings DE, et al. The mechanism of diabetes control after gastrointestinal bypass surgery reveals a role of the proximal small intestine in the pathophysiology of type 2 diabetes. Ann Surg. 2006;244:741–9.

Tables

Table 1: Analysis of circulating biomarkers.

	Control	ESG	NOTES-GB	P value
Age (Month) Mean	5.3	4.9	5.1	NS
Weight (Kg) Mean (SD)				
Week 0	33.7 (1.56)	37.3 (1.06)	35.8 (3.99)	0.013*
Week 4	45.2 (2.26)	48 (4.24)	39.7 (6.25)	
Week 12	58.1 (9.83)	58.5 (10.6)	63.5 (16.0)	
Week 24	71.7 (7.49)	76.5 (9.19)	73.9 (25.27)	
Week 28	78 (3.67)	79.5 (6.36)	69.5 (25.51)	
Procedure Duration (Min) Mean	10 (2.83)	68 (11.31)	215 (15.89)	<0.001*
ALT (U/L) Mean				NS
Week 0	54	70.5	46.7	
Week 4	48	75.5	46.5	
Week 12	49	60	41.7	
Week 24	42	60.5	48	
Week 28	38.5	52	56.2	
AST (U/L) Mean				NS
Week 0	63.5	36.5	32.7	
Week 4	43.5	34	27.5	
Week 12	42	36	29.3	
Week 24	29	53	31	
Week 28	28.5	48	34.4	
Insulin (mU/L) Mean				NS
Week 0	1.84	0.48	0.55	
Week 4	7.11	1.11	1.08	

Week 12	4.66	2.07	1.33	
Week 24	2.8	1.24	0.65	
Week 28	1.86	0.27	0.97	
Glucose (MMLO/L) Mean				NS
Week 0	5.2	5.2	5.12	
Week 4	3.65	4.4	4.72	
Week 12	4.65	4.55	4.67	
Week 24	4.6	4.1	4.45	
Week 28	4.25	3.7	4.34	
C-Peptide (UG/L) Mean				NS
Week 0	0.02	0.01	0.04	
Week 4	0.03	0.01	0.02	
Week 12	0.03	0.025	0.017	
Week 24	0.02	0.025	0.022	
Week 28	0.02	0.03	0.017	
Albumin (G/L) Mean				NS
Week 0	30	34	34.5	
Week 4	33.5	35.5	34.67	
Week 12	39	37.5	35.5	
Week 24	36.5	39.5	34.17	
Week 28	35	37	31.5	
GLP-1 (pM) Mean (SD)				0.011*
Week 0	2.78 (0.46)	4.162 (1.45)	5.844 (1.91)	
Week 4	7.32 (1.23)	5.73 (2.05)	6.067 (2.09)	
Week 12	3.9 (0.08)	5.487 (2.44)	5.791 (3.79)	
Week 24	3.54 (0.74)	2.03 (1.03)	5.405 (3.87)	

Week 28	2.95 (1.63)	1.727 (0.34)	8.53 (6.06)	
Fructosamine (UMOL/L) Mean				NS
Week 0	212.5	235.5	135.3	
Week 4	234	232	223.3	
Week 12	266.5	245	229.2	
Week 24	268	262	238.8	
Week 28	273	263.5	228.5	
HbA1c (%) Mean				NS
Week 0	4.2	4.2	4.1	
Week 4	4.2	4.2	4.2	
Week 12	4.2	4.2	4.2	
Week 24	4.2	4.2	4.2	
Week 28	4.1	4.2	4.1	
Hb (g/dL) Mean (SD)				NS
Week 0	10.25 (0.78)	10.25 (0.35)	10.7 (1.25)	
Week 4	11.35 (0.35)	10.6 (0.01)	11.31 (1.09)	
Week 12	11.7 (1.27)	12.75 (1.62)	11.27 (1.79)	
Week 24	12.85 (0.49)	13.05 (0.49)	10.45 (2.97)	
Week 28	12.6 (0.28)	11.5 (0.28)	9.95 (3.56)	

Figures

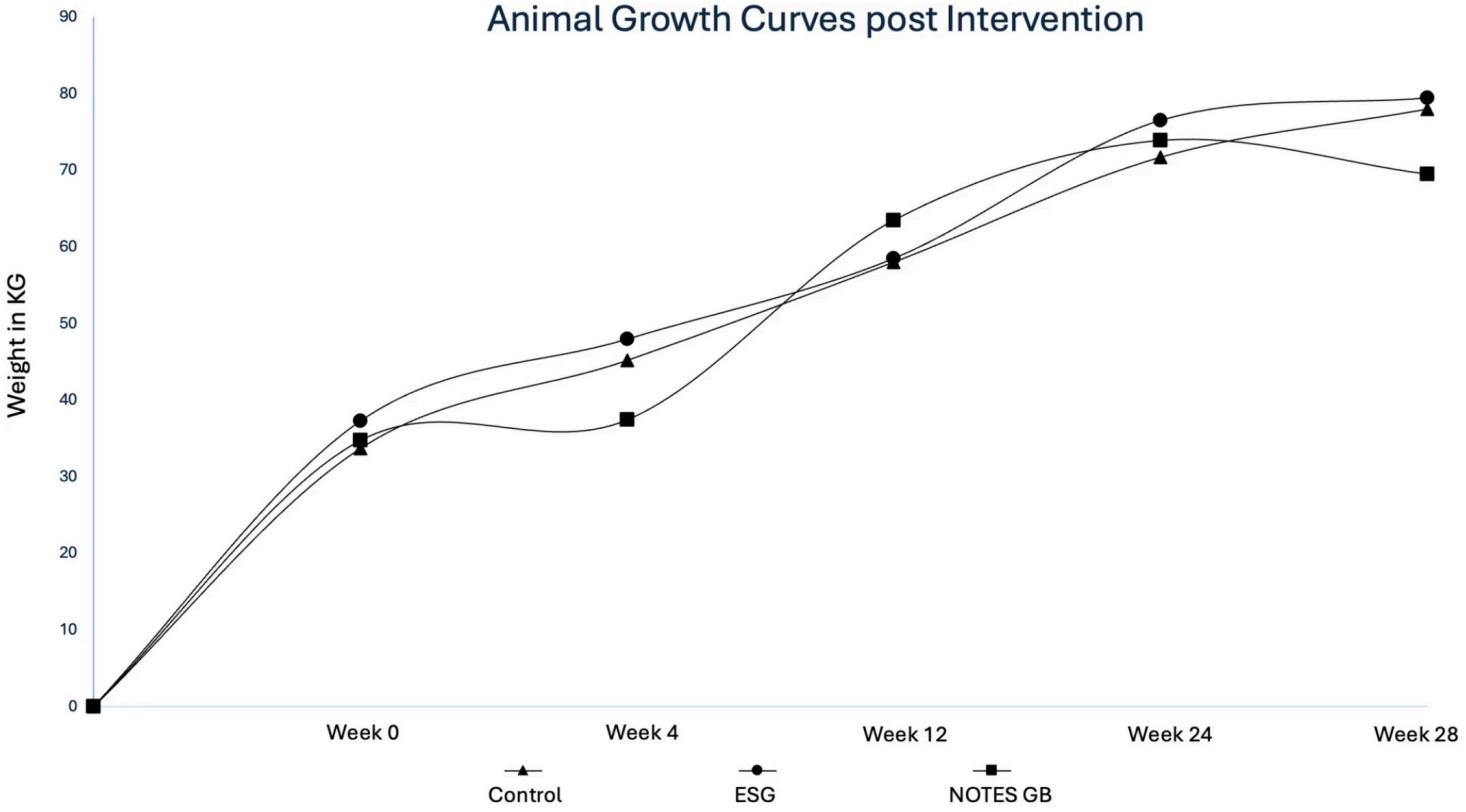


Figure 1

Comparing animal growth curves between control, ESG, and NOTES-GB.

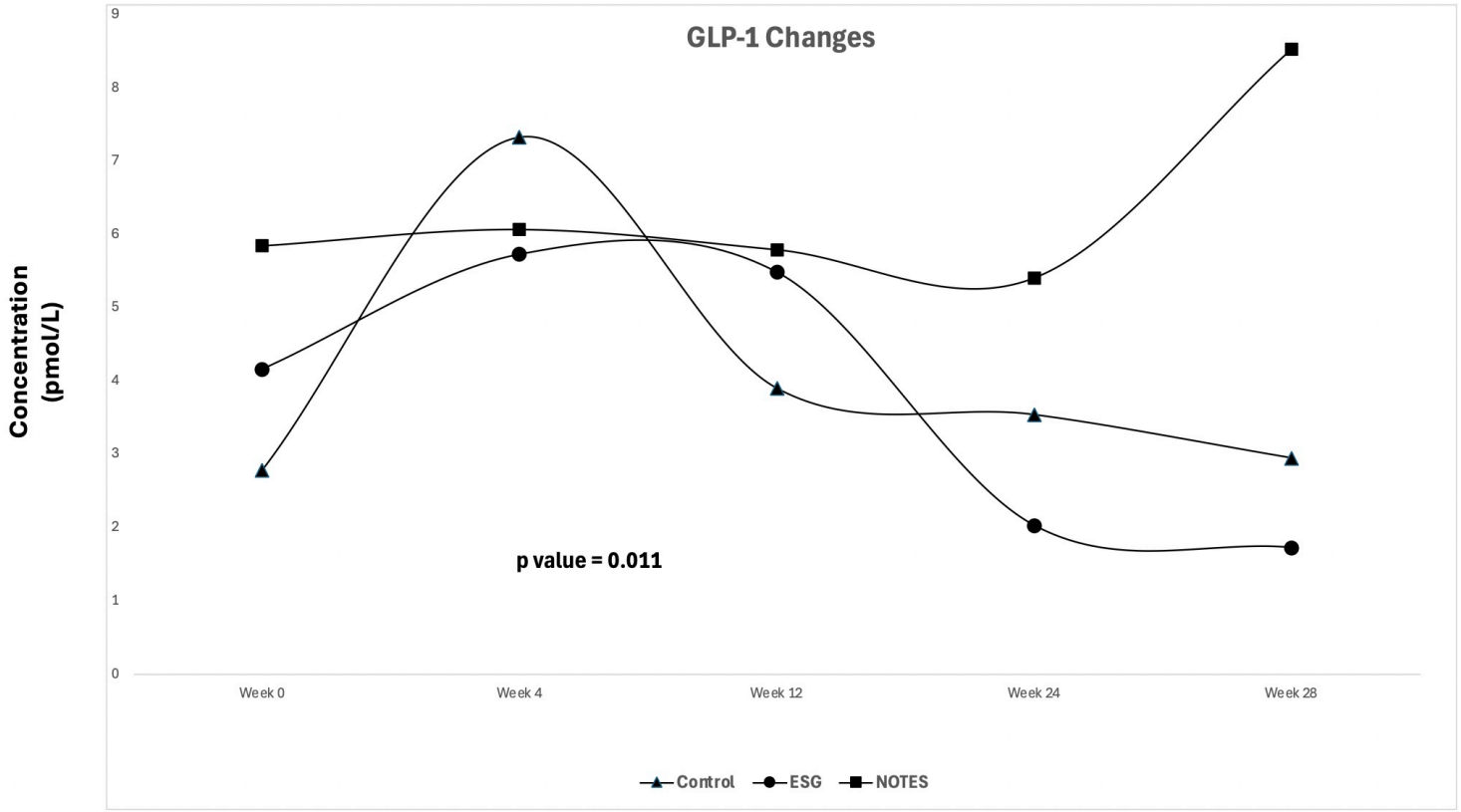


Figure 2

Plasma fasting GLP-1 level between control, ESG and NOTES-GB.

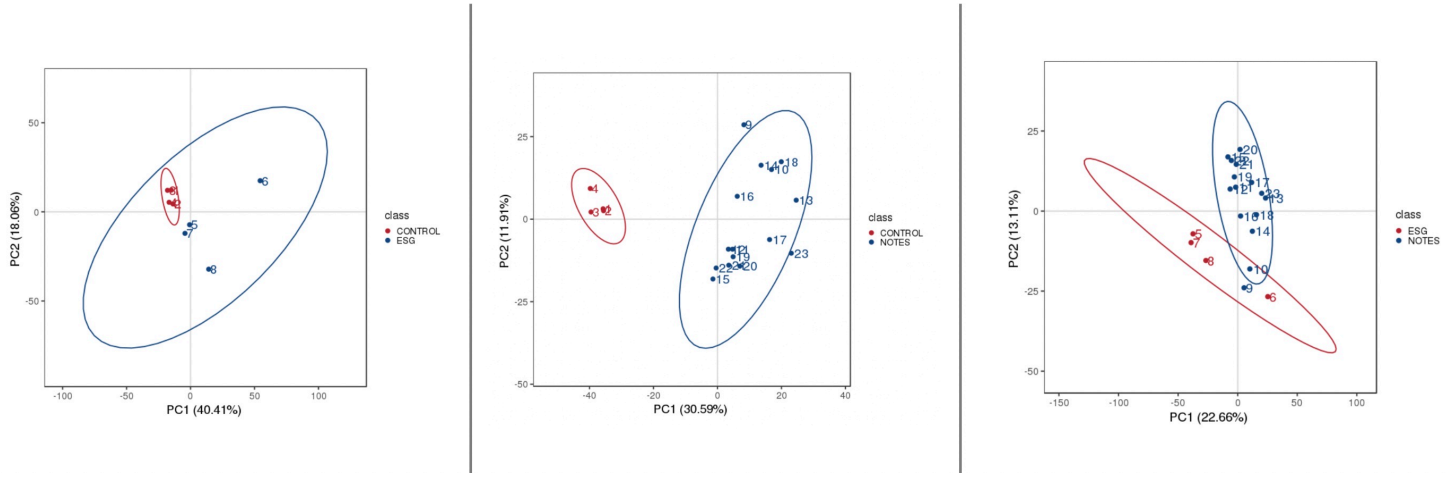


Figure 3

Principal component analysis (PCA). The abscissa PC1 and ordinate PC2 represent the scores of the first and second principal components, respectively. Scatters of different colors represent samples from different experimental groups. The ellipse is 95% confidence interval.

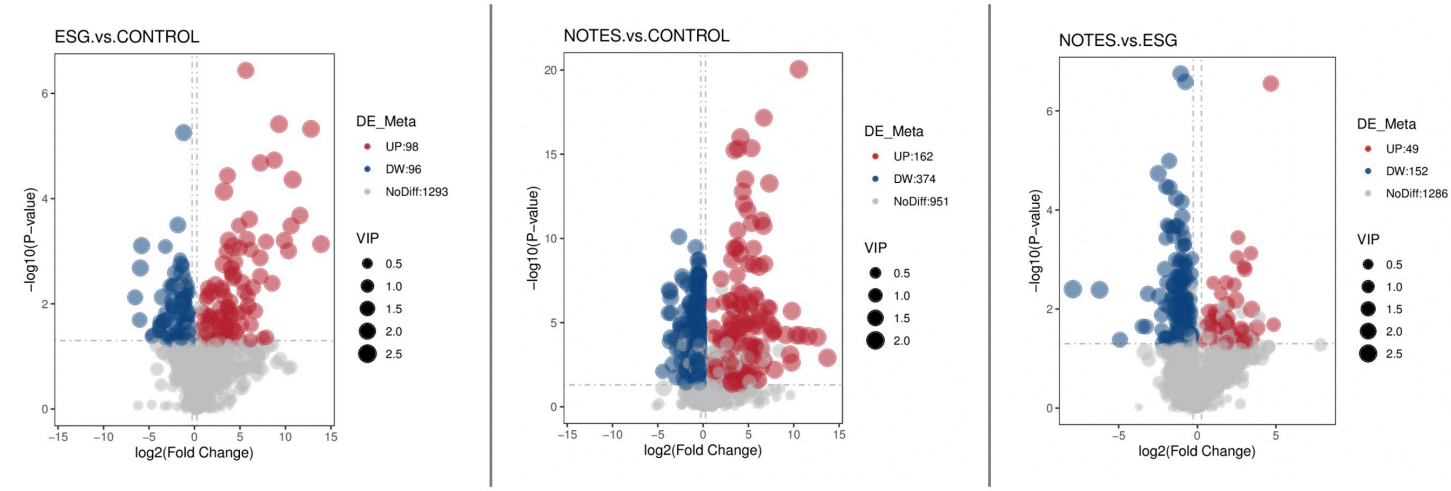


Figure 4

Volcano plot of differential metabolites. Each point in the volcano plot represents a metabolite, the significantly up-regulated metabolite is represented by a red dot, the significantly down-regulated metabolite is represented by a blue dot, and the size of the dot represents the VIP value.

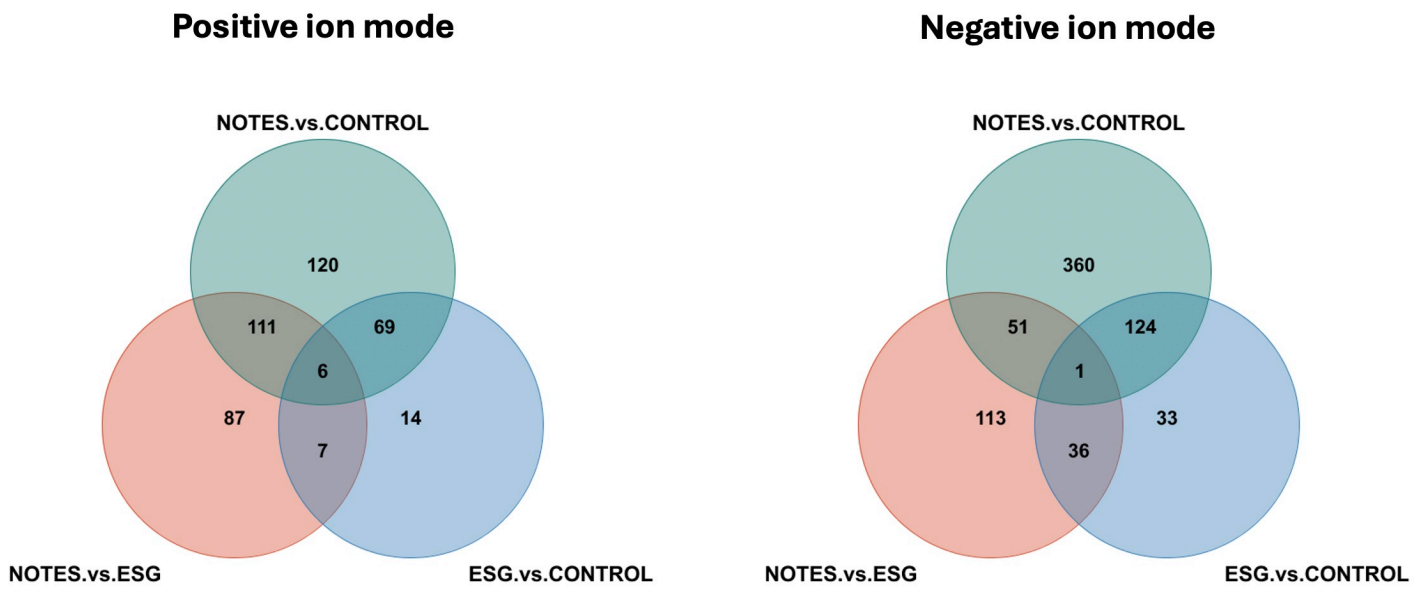


Figure 5

Venn diagram compare the overlap and unique difference metabolites between different groups.

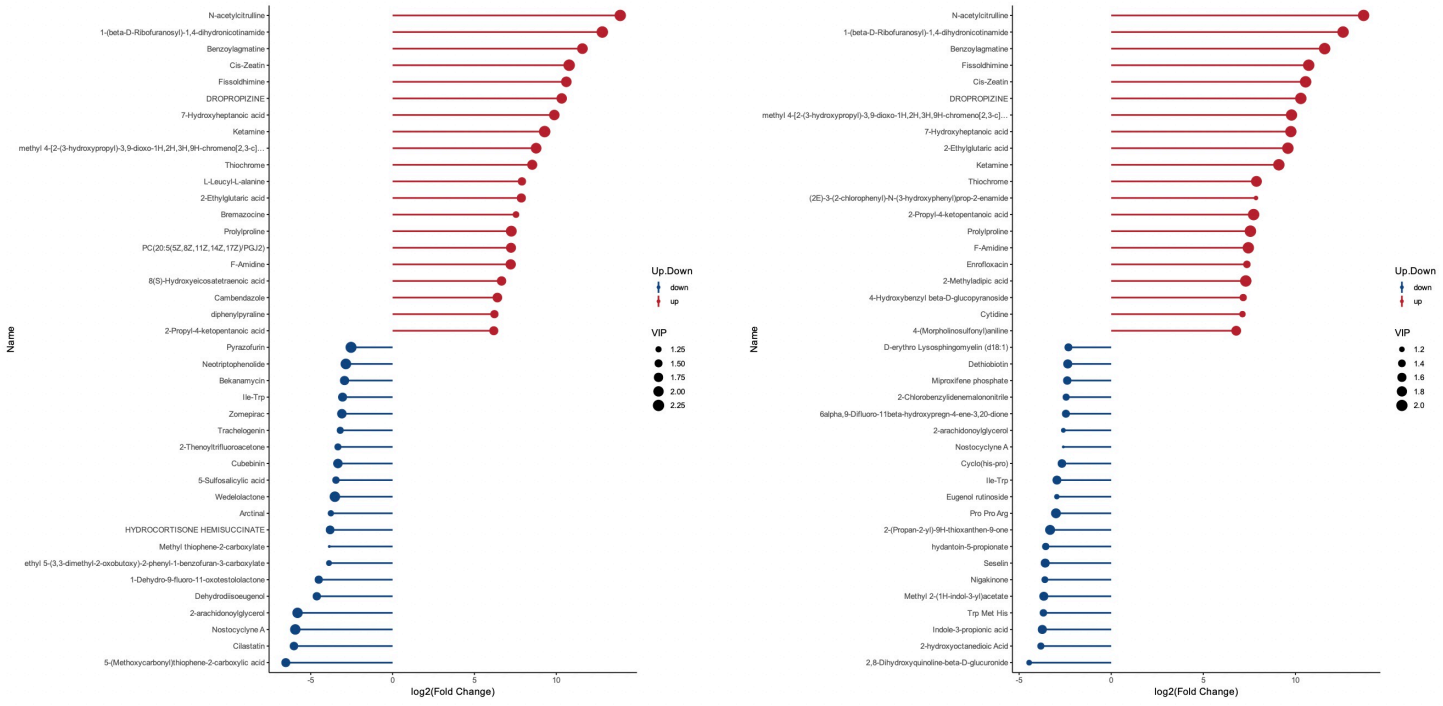


Figure 6

Matchstick plot of differential metabolites clearly show the up and down-regulation of the metabolites and the substances with large difference multiples. The color of the dot represents the up and down-

regulation, the length of the rod represents the size of log2 (Fold Change); The size of the point represents the size of the VIP value.

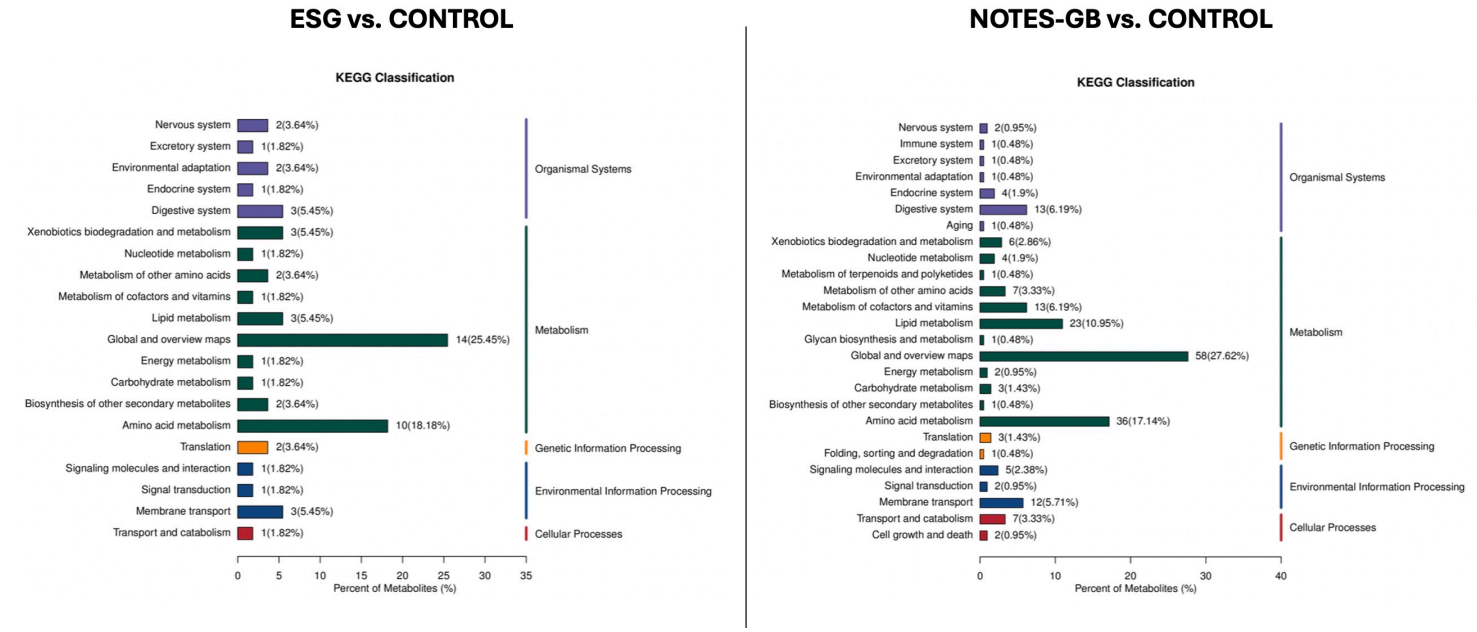


Figure 7

The Kyoto Encyclopedia of Genes and Genomes (KEGG) classification chart was plotted based on the differential metabolites from two different groups. The horizontal coordinates in the graph indicate the number of metabolites annotated under a particular KEGG pathway as a percentage of the number of all annotated metabolites, the vertical coordinates are KEGG pathway primary classifications on the right and KEGG pathway secondary classifications on the left.

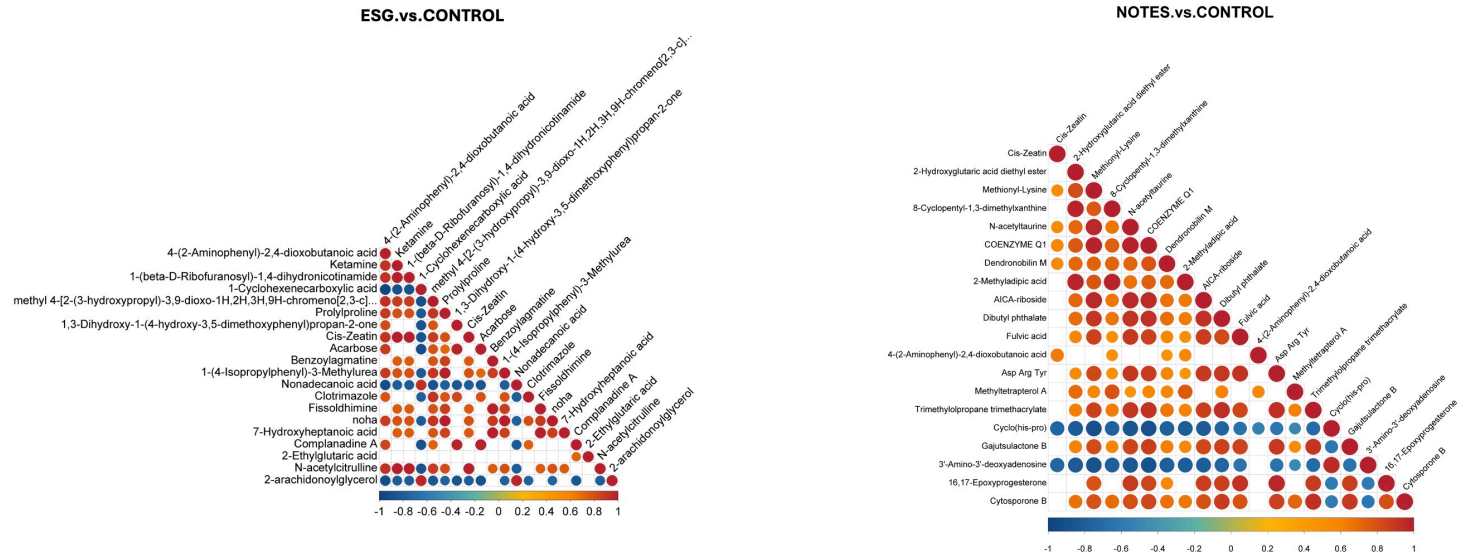


Figure 8

Correlation diagram of differential metabolites. The highest correlation is 1, which is a complete positive correlation (red), and the lowest correlation is -1, which is a complete negative correlation (blue). The part without color indicates P-value > 0.05. The figure shows the correlation of the differential metabolites of top 20 sorted by P-value from small to large.